

Original Article



Intranasal Immunization With Nanoparticles Containing an *Orientia tsutsugamushi* Protein Vaccine Candidate and a Polysorbitol Transporter Adjuvant Enhances Both Humoral and Cellular Immune Responses

OPEN ACCESS

Received: Jun 1, 2023

Revised: Dec 8, 2023

Accepted: Dec 10, 2023

Published online: Dec 15, 2023

*Correspondence to

Hyuk Chu

Division of Zoonotic and Vector Borne Disease Research, Center for Infectious Disease Research, National Institute of Health, 187 Osongsaengmyeong 2-ro, Osong-eup, Heungdeok-gu, Cheongju 28159, Korea.
Email: chuhyuk@korea.kr

Cheol-Heui Yun

Department of Agricultural Biotechnology, and Research Institute of Agriculture and Life Sciences, Seoul National University, 1 Gwanak-ro, Gwanak-gu, Seoul 08826, Korea.
Email: cyun@snu.ac.kr

Copyright © 2023. The Korean Association of Immunologists

This is an Open Access article distributed under the terms of the Creative Commons Attribution Non-Commercial License (<https://creativecommons.org/licenses/by-nc/4.0/>) which permits unrestricted non-commercial use, distribution, and reproduction in any medium, provided the original work is properly cited.

ORCID iDs

Cheol Gyun Kim

<https://orcid.org/0009-0007-8384-037X>

Won Kyong Kim

<https://orcid.org/0000-0003-3015-0416>

Narae Kim

<https://orcid.org/0000-0003-4216-0857>

Cheol Gyun Kim ^{1,2}, Won Kyong Kim ³, Narae Kim ¹, Young Jin Pyung ¹, Da-Jeong Park ¹, Jeong-Cheol Lee¹, Chong-Su Cho¹, Hyuk Chu ^{3,*}, Cheol-Heui Yun ^{1,4,5,6,*}

¹Department of Agricultural Biotechnology, and Research Institute of Agriculture and Life Sciences, Seoul National University, Seoul 08826, Korea

²Bio-MAX/N-Bio, Seoul National University, Seoul 08826, Korea

³Division of Zoonotic and Vector Borne Disease Research, Center for Infectious Disease Research, National Institute of Health, Cheongju 28159, Korea

⁴Center for Food and Bioconvergence, Seoul National University, Seoul 08826, Korea


⁵Institutes of Green-bio Science and Technology, Seoul National University, Pyeongchang 25354, Korea

⁶Interdisciplinary Programs in Agricultural Genomics, Seoul National University, Seoul 08826, Korea


ABSTRACT

Scrub typhus, a mite-borne infectious disease, is caused by *Orientia tsutsugamushi*. Despite many attempts to develop a protective strategy, an effective preventive vaccine has not been developed. The identification of appropriate Ags that cover diverse antigenic strains and provide long-lasting immunity is a fundamental challenge in the development of a scrub typhus vaccine. We investigated whether this limitation could be overcome by harnessing the nanoparticle-forming polysorbitol transporter (PST) for an *O. tsutsugamushi* vaccine strategy. Two target proteins, 56-kDa type-specific Ag (TSA56) and surface cell Ag A (ScaA) were used as vaccine candidates. PST formed stable nano-size complexes with TSA56 (TSA56-PST) and ScaA (ScaA-PST); neither exhibited cytotoxicity. The formation of Ag-specific IgG2a, IgG2b, and IgA in mice was enhanced by intranasal vaccination with TSA56-PST or ScaA-PST. The vaccines containing PST induced Ag-specific proliferation of CD8⁺ and CD4⁺ T cells. Furthermore, the vaccines containing PST improved the mouse survival against *O. tsutsugamushi* infection. Collectively, the present study indicated that PST could enhance both Ag-specific humoral immunity and T cell response, which are essential to effectively confer protective immunity against *O. tsutsugamushi* infection. These findings suggest that PST has potential for use in an intranasal vaccination strategy.

Keywords: *Orientia tsutsugamushi*; Intranasal administration; Nano-vaccine; Adaptive immunity

Young Jin Pyung 


<https://orcid.org/0000-0001-8313-8475>

Da-Jeong Park 

<https://orcid.org/0000-0002-0560-0158>

Hyuk Chu 

<https://orcid.org/0000-0002-7044-2942>

Cheol-Heui Yun 

<https://orcid.org/0000-0002-0041-2887>

Conflict of Interest

The authors declare no potential conflicts of interest.

Abbreviations

¹H NMR, proton nuclear magnetic resonance; 7-AAD, 7-amino-actinomycin; APC, Ag presenting cell; BMDC, bone marrow-derived dendritic cell; CTV, cell trace violet; DC, dendritic cell; DLS, dynamic light scattering; ICU, infected cell-counting unit; KCDC, Korea Centers for Disease Control and Prevention; LMW, low molecular weight; OVA, ovalbumin; PEI, polyethylenimine; PST, polysorbital transporter; ScaA, surface cell Ag A; SDA, sorbitol diacrylate; TSA56, 56-kDa type-specific Ag.

Author Contributions

Conceptualization: Kim CG, Chu H, Yun CH; Data curation: Kim CG, Lee JC; Formal analysis: Kim CG, Kim WK; Funding acquisition: Chu H, Yun CH; Investigation: Kim CG, Kim WK, Kim N, Pyung YJ, Park DJ, Lee JC, Cho CS; Methodology: Kim CG, Kim WK, Kim N, Pyung YJ, Park DJ, Lee JC, Cho CS; Resources: Kim WK, Kim N, Pyung YJ, Park DJ, Lee JC, Cho CS; Supervision: Chu H, Yun CH; Writing - original draft: Kim CG; Writing - review & editing: Kim WK, Chu H, Yun CH.

INTRODUCTION

Scrub typhus is an acute, feverish, and sometimes fatal disease that is caused by infection with the obligate intracellular bacterium, *Orientia tsutsugamushi*. It has become a serious public health concern. It is frequently observed in the Asia-Pacific region, often referred to as the “tsutsugamushi triangle” (1). Sporadic outbreaks have also been reported (2). Recent epidemiological studies have shown that scrub typhus is spreading outside of its typical endemic areas; thus, scrub typhus is becoming a global problem (3,4). Unfortunately, a reliable prophylactic vaccine has not been developed against *O. tsutsugamushi*, despite numerous attempts to develop a protective strategy in recent decades (5-7). Because of poor cross-reactivity among *O. tsutsugamushi* genotypes, the protective immunity produced by early vaccine trials or natural infection does not persist. The greatest obstacles to the development of a scrub typhus vaccine include the identification of vaccine candidates that cover a broad range of antigenic strains with long-lasting immunity (8,9).

Various attempts to select appropriate vaccine candidates have led to further investigations with the aim of developing a better vaccine (10,11). The difficulties of using live or killed *O. tsutsugamushi* as a scrub typhus vaccine include the need for large-scale manufacturing. Because of the requirement for a biosafety level-3 laboratory space, manufacturing is inconvenient and costly. Thus, scrub typhus vaccine strategies have mainly focused on subunit vaccines using recombinant protein (11). In the present study, we used surface cell Ag A (ScaA) acting as an adhesin molecule that could confer protective immunity when used as vaccine candidate in a mouse model infected with *O. tsutsugamushi* (8,12). We also used a highly immunogenic outer membrane protein, 56-kDa type-specific Ag (TSA56), which plays an important roles in *O. tsutsugamushi* attachment and invasion to the host cells. Furthermore, when used as a vaccine candidate protein, TSA56 plays a role in genetic and antigenic heterogeneity (13,14).

Nanotechnology has made significant contributions to vaccine development, particularly with respect to delivery and adjuvanticity. The physicochemical characteristics of nanovaccines (e.g., size, viscosity, and surface charge) contribute to their efficacy by modulating the retention of vaccine in target tissues and mobility in lymphatic and blood vessels (15,16). The size of a nanovaccine is advantageous for targeting lymph nodes because 10–100 nm particles can easily move through the interstitium and enter the lymphatic system, rather than blood vessels (17,18). Strategies to modulate intracellular Ag mobility for the induction of CD8⁺ T cell responses have also been devised using nanotechnology (18). Polysorbital transporter (PST), synthesized from low-molecular-weight (LMW) polyethylenimine (PEI) and sorbitol diacrylate (SDA), has demonstrated long-term Ag-specific Ab production against respiratory syncytial virus infection (19) and pneumococcal pneumonia, along with follicular helper T cell activation (20). Notably, PST is assumed to induce robust humoral and cellular immune responses.

Because *O. tsutsugamushi* is an intracellular parasitic bacterium, the infection cannot be effectively controlled by Ab production alone. This is a primary reason for difficulty during protective vaccine development against virus (21) or intracellular bacteria (9,22). Thus, there is a need for Ag-specific CD8⁺ T cell responses that can directly kill infected cells, in combination with the production of neutralizing Abs (23,24). In the present study, we found that a vaccine strategy harnessing nanoparticle-forming PST could elicit enhanced Ab production, along with Ag-specific T cell responses, to achieve protective immunity against *O. tsutsugamushi* infection.

MATERIALS AND METHODS

Experimental animals

Female BALB/c mice (6–10 wk old) were purchased from RaonBio Inc. (Yongin, Korea). Mice were maintained under pathogen-free conditions in an animal facility at Seoul National University, and procedures were performed with the approval of the Institutional Animal Care and Use Committee (IACUC; approval No. SNU-200416-5-5). All challenge experiments using *O. tsutsugamushi* were conducted in the animal biosafety level-3 facility of the Korea Centers for Disease Control and Prevention (KCDC), with the approval of the IACUC at the KCDC in accordance with the laboratory's animal ethics guidelines (KDCA-IACUC-21-011). The animal care and use protocol for the present study adhered to guidelines established by the Korea Association for Laboratory Animal Sciences.

Cell culture

Vero (ATCC CCL-81) and L929 (ATCC NCTC929) cells were maintained in DMEM (Gibco, Grand Island, NY, USA) supplemented with 5% heat-inactivated FBS (Gibco), 100 U/ml penicillin, and 100 µg/ml streptomycin (Gibco); cells were incubated at 37°C with 5% CO₂.

Preparation of TSA56 and ScaA proteins

For the preparation of TSA56 and ScaA proteins, corresponding bacterial genes were amplified from the genomic DNA of the *O. tsutsugamushi* Boryong strain via polymerase chain reaction using the primer pairs TSA56 (forward primer: 5'-CGGGATCCGATCCATCAGCTTCA TCA-3', reverse primer: 5'-CGGTCGACTATATCTTCGTCTTTGCC-3') and ScaA (forward primer: 5'-CGGGATCCGCACCAGGATTTAGAAGCA-3', reverse primer: 5'-CGGTCGACTTTA CTTGATTCTTTGC-3'). The polymerase chain reaction products were cloned into pET28a vector (Novagen, Gibbstown, NJ, USA). All constructs were sequenced to confirm in-frame cloning (data not shown). Recombinant TSA56 and ScaA proteins were purified from a recombinant plasmid containing *Escherichia coli* BL21 (DE3) cultured overnight at 37°C in Luria–Bertani medium supplemented with 50 µg/ml kanamycin (Sigma-Aldrich, St. Louis, MO, USA). Each culture was transferred into fresh Luria–Bertani medium and incubated until it reached an OD₆₀₀ of 0.5–1.0. Protein expression in transformed *E. coli* was enhanced by incubation with isopropyl β-D-thiogalactoside (0.1 mM; Duchefa, Zwijndrecht, Netherlands) at 37°C for 4 h, then harvested by centrifugation at 4,000 ×g for 10 min. The resulting pellets were suspended in PBS and sonicated; soluble fractions were then separated by centrifugation at 20,000 ×g for 30 min. The proteins were purified using Ni-nitrilotriacetic acid His-resin (Qiagen, Carlsbad, CA, USA) or a glutathione-sepharose 4B column (GE Healthcare, Piscataway, NJ, USA), in accordance with the manufacturer's instructions. The purified proteins were dialyzed against PBS in an Aside-A-Lyzer Dialysis Cassette (Thermo Fisher Scientific, Rockford, IL, USA) at 4°C overnight. Then, purified proteins were treated with endotoxin removal column (Thermo Fisher Scientific); endotoxin contamination was determined using an Endosafe PTS cartridge (Cat # PTS20F, 1.0–0.0; Charles River, Wilmington, MA, USA), in accordance with the manufacturer's instructions. All purified proteins contained <100 EU/mg of endotoxin (data not shown).

Synthesis of PST

PST was synthesized with SDA and LMW (600 Da) PEI by a Michael addition reaction as previously described (19,20), with a slight modification. Briefly, SDA and PEI were separately dissolved in DMSO at concentration of 0.836 M and 0.209 M, respectively. The SDA solution was then added dropwise to PEI while gently stirring at a feed molar ratio of SDA:PEI =

4:1. The reaction mixture was continuously stirred at 80°C for 24 h, then dialyzed (using a Spectra/Pro® membrane with 3500 Da molecular weight cut-off) against distilled water at 4°C, lyophilized, and stored at -70°C until use.

Physicochemical characterization of the TSA56-PST and ScaA-PST complexes

The ability of PST to complex with ovalbumin (OVA) was determined by dynamic light scattering (DLS). Briefly, TSA56-PST or ScaA-PST complexes were prepared at various weight ratios by incubating the components at room temperature for 30 min with a final protein concentration of 500 µg/ml. The particle sizes of the TSA56-PST and ScaA-PST complexes were measured by a DLS spectrophotometer (DLS-7000; Otsuka Electronics, Osaka, Japan).

Generation and culture of bone marrow-derived dendritic cells (BMDCs)

BMDCs were generated from murine bone marrow cells as previously described (25). Briefly, bone marrow was flushed from the tibiae and femurs of B6 mice, then depleted of red blood using red blood cell-lysis buffer (Sigma-Aldrich). The resulting bone marrow cells were cultured in complete RPMI medium with 20 ng/ml GM-CSF (Creagene, Seongnam, Korea) at 37°C with 5% CO₂ for 7 days. Complete RPMI medium was composed of RPMI-1640 supplemented with 10% FBS, 20 mM HEPES, 1 mM sodium pyruvate, 220 nM 2-mercaptoethanol, and 100 µg/ml gentamicin (all from Sigma-Aldrich). On day 0, bone marrow cells were seeded at 3×10⁶ cells/well (3 ml media) in a six-well plate; 2 ml of fresh media were added on day 3. On day 5, half of the culture supernatant was discarded, and 3 ml of fresh media were added. On day 7, suspended bone marrow cells were harvested and sorted using a CD11c MicroBeads UltraPure kit (Miltenyi Biotec Inc., San Jose, CA, USA). Differentiation into dendritic cells (DCs) was confirmed by staining with anti-CD11c and - MHC class II Abs (BD Biosciences, Franklin Lakes, NJ, USA) via flow cytometry (FACS CantoII; BD Biosciences).

Cytotoxicity assay

To examine cytotoxicity, BMDCs were treated with TSA56-PST or ScaA-PST complexes at various doses for 24 h. After FC-receptors had been blocked with anti-CD16/32 Abs (eBioscience, San Diego, CA, USA), the cells were stained with CD11c, MHC class II, MHC class I, and annexin V/7-amino-actinomycin (7-AAD; BD Biosciences) at 4°C for 20 min, then examined for cytotoxicity. The cells were examined by flow cytometry (FACS CantoII, BD Biosciences); all cytometric data were analyzed using FlowJo software (Flowjo, Ashland, OR, USA).

Immunization with TSA56- or ScaA-PST complex vaccines

Mice were intranasally immunized with 10 µg (20 µl in PBS/mouse) of TSA56, ScaA, TSA56-PST, or ScaA-PST complexes (weight ratio 1:10), three times at 2-wk intervals. To determine Ag-specific Ab levels in serum, retro-orbital blood samples were collected four times at 2-wk intervals beginning on the day before initial vaccination.

Measurement of Ab responses by ELISA

ELISA was performed to evaluate immune responses against TSA56 and ScaA proteins in serum samples from immunized mice. Briefly, 96-well microtiter plates (Nunc, Roskilde, Denmark) were coated overnight with pre-titrated recombinant TSA56 (3 µg/ml) or ScaA (3 µg/ml) proteins in PBS, blocked with PBS containing 3% skim milk (200 µl/well) for 30 min, and washed with PBS containing 0.05% Tween-20. Serum samples were diluted at 1:100 in PBS containing 3% skim milk. Horseradish peroxidase-conjugated goat anti-mouse IgG or IgA Ab (Bethyl Lab Inc., Montgomery, TX, USA) was added to each well. Enzymatic reactions

were conducted by adding substrate containing o-phenylenediamine (Sigma-Aldrich) and optical density was examined using an automated ELISA spectrophotometer (Multiskan GO; Thermo Fisher Scientific) at 450 nm. Ab concentrations were determined after readings had been normalized with respect to the plate background.

Ag restimulation assay

To investigate Ag-specific T cell responses, spleens were collected 2 wk after the third vaccination; single cells from splenocytes were labeled with 5 μ M cell trace violet (CTV; Invitrogen, Carlsbad, CA, USA). Then, CTV-labeled splenocytes (1×10^6 cells/well) were restimulated with TSA56 or ScaA protein at 10 μ g/ml for 72 h. Changes in T cell proliferation and population were examined by CTV and surface staining by anti-CD3, -CD8, and -CD4 Abs (BD Biosciences) using flow cytometry (FACS CantoII; BD Biosciences). All cytometric data were analyzed using FlowJo software.

O. tsutsugamushi propagation and challenge

The *O. tsutsugamushi* Boryong strain was propagated in the monolayer of L929 cells as previously described (26). Briefly, bacteria were inoculated into confluent monolayer of the cells in FBS-free DMEM (Gibco) and incubated at 34 °C for 2 h, at the end of which DMEM was then supplemented with 1% FBS and 1% HEPES (Invitrogen). The levels of infectivity were determined by an indirect immunofluorescence assay. When >90% of cells were infected, the cells were collected, homogenized using a glass Dounce homogenizer (Wheaton Industries Inc., Millville, NJ, USA) and centrifuged at 500 \times g for 5 min. The supernatant was stored in liquid nitrogen tank until use. The infected cell-counting unit (ICU) was calculated by microscopic analysis, according to the following formula: ICU = Total Number of Cells Used for Infection \times Ratio of Infected Cells to Counted Cells \times Dilution Fold of *O. tsutsugamushi* Boryong Inoculum (27,28). A 100% lethal dose of *O. tsutsugamushi* was determined as 5×10^6 ICU in wild type BALB/c mice. For the challenge experiments, immunized BALB/c mice were intraperitoneally infected with a 100% lethal dose of *O. tsutsugamushi* Boryong strain in 200 μ l of PBS at 14 days after the last immunization. Mice were monitored daily for signs of morbidity based on body weight changes and mortality for 21 days. Body weight loss >30% was regarded as the experimental endpoint.

Statistical analysis

The levels of statistical significance for comparisons between samples were determined by *t*-tests or one or two-way ANOVA test by using GraphPad InStat software (version 8; GraphPad, San Diego, CA, USA). The results were expressed as the mean \pm SEM. The threshold for statistical significance was regarded as $p < 0.05$.

RESULTS

PST and target recombinant proteins from *O. tsutsugamushi* were successfully synthesized

PST was synthesized from SDA and LMW PEI (600 Da) by the Michael addition reaction, as previously described (19,20). When PST, is properly formed, it has various functional properties including degradation, a proton sponge effect, and osmotic activity (Fig. 1A). The composition of the synthesized PST was determined by proton nuclear magnetic resonance (1 H NMR) spectroscopy (Fig. 1B). Its ester bond maintains the biodegradability of PST (19), ensuring safety. When the 1 H NMR spectra of SDA, LMW PEI, and PST were compared, the peaks of acrylate

Protective Immunity Induced by Intranasal Nano-Vaccine

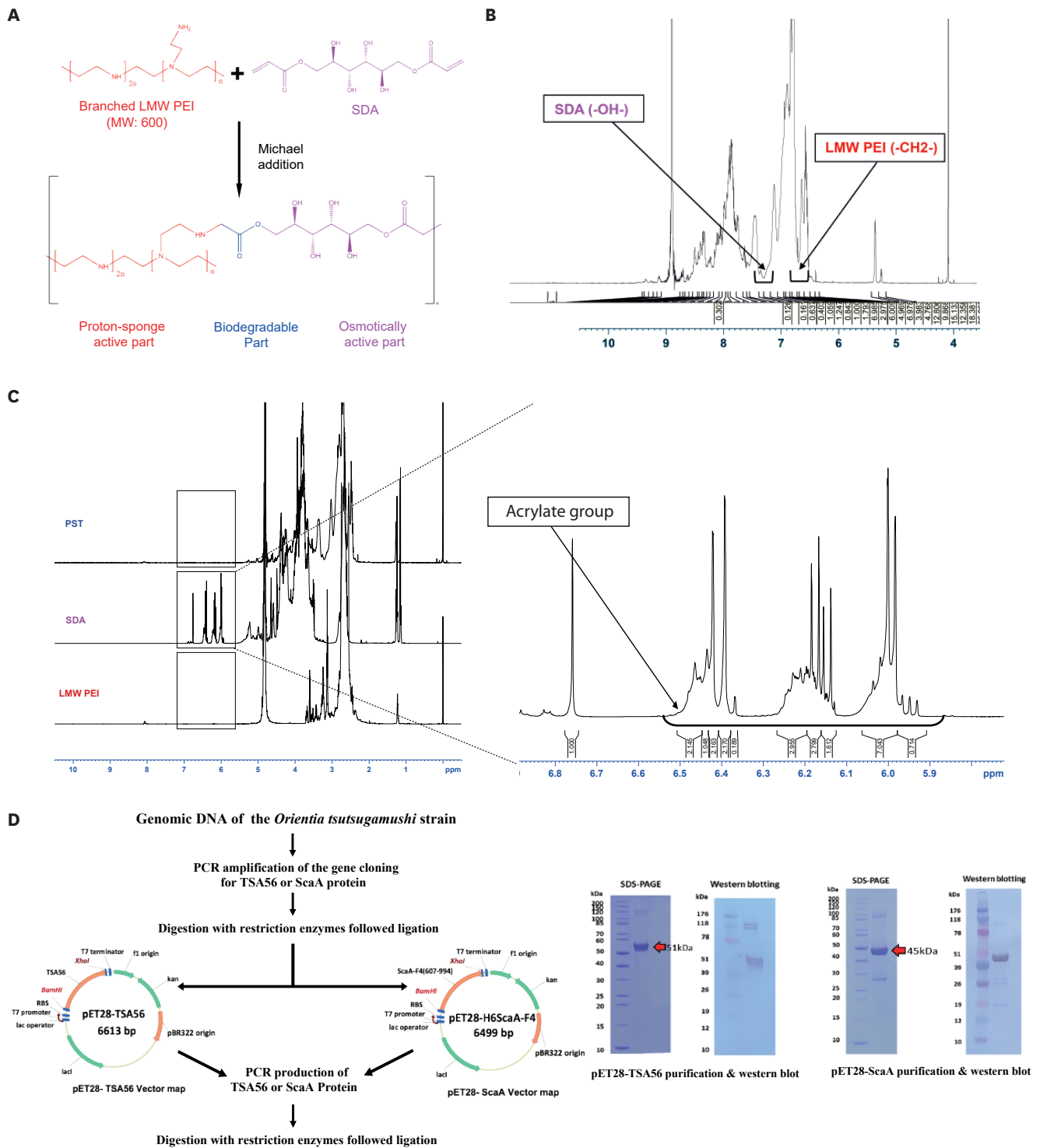


Figure 1. Synthesis of PST and cloning of recombinant proteins from *Orientia tsutsugamushi*. (A) Reaction scheme for PST preparation via a Michael reaction between SDA and branched LMW PEI (feed molar ratio of SDA:PEI = 4:1). (B) ^1H NMR spectrum of PST. (C) Comparison of ^1H NMR spectra among SDA, branched LMW PEI, and PST. Frame near 6–7 ppm indicates acrylate groups. Acrylate groups of SDA are shown enlarged on the right side of the panel. (D) Target recombinant proteins, TSA56 and ScaA, were synthesized using *E. coli* and a pET28 cloning vector system. Truncated forms of recombinant TSA56 (amino acids 88–479) and ScaA (amino acids 607–994) were produced. Expected sizes of synthesized proteins were confirmed by Coomassie blue staining and western blotting.

groups were observed between 5.9 and 6.5 ppm, but they were absent after the synthesis of PST by the Michael addition reaction with PEI and SDA (**Fig. 1C**). These results indicated that biodegradable ester bonds were formed during the synthesis of PST. Synthesis of the target recombinant proteins, TSA56 and ScaA, using an *E. coli* and pET28a cloning vector system was confirmed by Coomassie blue staining and western blotting (**Fig. 1D**). Collectively, the results indicated that PST and the target proteins, TSA56 and ScaA were successfully prepared.

Non-cytotoxic complexes of PST with each target Ag were formed with the expected size and stability

Nanoparticle sizes have key roles in nanovaccine efficacy and delivery (19,20). A nanovaccine particle size of 20–200 nm is reportedly favorable for endocytosis by Ag presenting cells (APCs) that initiate and/or induce the activation of T cell responses; microparticles in the size range of 0.5–5 μm are internalized by phagocytosis, thus favoring a humoral immune response (18). To determine the optimal conditions for the formation of nanocomplexes with the TSA56 and ScaA target proteins, PST was mixed with each Ag at weight ratios of 1:1, 1:5, and 1:10, resulting in nanoparticle formation. Nanoparticle size was analyzed by DLS. Both target proteins had an appropriate nanoparticle size of 100–200 nm at a ratio of 1:10 (**Fig. 2A and B**). The cytotoxicity of TSA56-PST and ScaA-PST were analyzed in BMDCs by using annexin V/7-AAD. Compared with a positive control; H_2O_2 treatment group, each nanocomplexes did not induce significant early apoptosis (Annexin V⁺7-AAD⁻) and necrosis (7-AAD⁺) (**Fig. 2C and D**). Collectively, the results indicated that PST optimally complexed with the TSA56 or ScaA proteins at a ratio of 1:10, without inducing cytotoxicity.

Nano-complexed TSA56 and ScaA Ags with a PST induced effective Ag-specific Ab response

To examine Ag-specific humoral immunity, we vaccinated the mice with TSA56, ScaA, TSA56-PST, or ScaA-PST three times at 2-wk intervals (**Fig. 3A**). Both groups vaccinated with TSA56-PST or ScaA-PST showed significant enhancement of Ag-specific responses after the second vaccination (**Fig. 3B and C**), with further enhancement after the third vaccination. When vaccination was conducted with Ag alone (in the absence of nanocomplexes formation), the Ab response was minimally affected. The level of Ag-specific IgA, which plays a key role in mucosal protective immunity, significantly increased after the third vaccination with TSA56-PST or ScaA-PST (**Fig. 3D**). These results suggested that vaccination with a nano-complexed *O. tsutsugamushi* target protein produced with PST could enhance Ag-specific humoral immunity.

Nano-complexed TSA56 and ScaA Ags produced with PST induced an effective Ag-specific T cell response

O. tsutsugamushi is an intracellular bacterium; thus, both Ag-specific Ab responses and cellular immune responses (e.g., T cell proliferation and IFN- γ expression) are critical for protective immunity (29-31). Two weeks after the third vaccination, spleens were collected, and single cells were labeled with CTV and changes in CD4⁺ and CD8⁺ T cell populations were examined after restimulation with TSA56 or ScaA proteins for 72 h (**Fig. 4A**). When the splenocytes were restimulated with the TSA56 (**Fig. 4B**) or ScaA (**Fig. 4C**) proteins, the overall proportions of CD8⁺ and CD4⁺ T cells did not change, presumably because of the low number of Ag-specific memory T cells (32-34). Therefore, we examined CTV and CD44 expression for memory cells responding to each of the restimulation Ags. To note that the memory T cells generated by vaccination could respond to TSA56 or ScaA protein, respectively, which is identified by CTV^{lo} and CD44⁺ expression (**Fig. 4A**). As a result, both the proliferation of Ag-specific CD4⁺ and CD8⁺ T cells restimulated with TSA56 protein was significantly enhanced in the

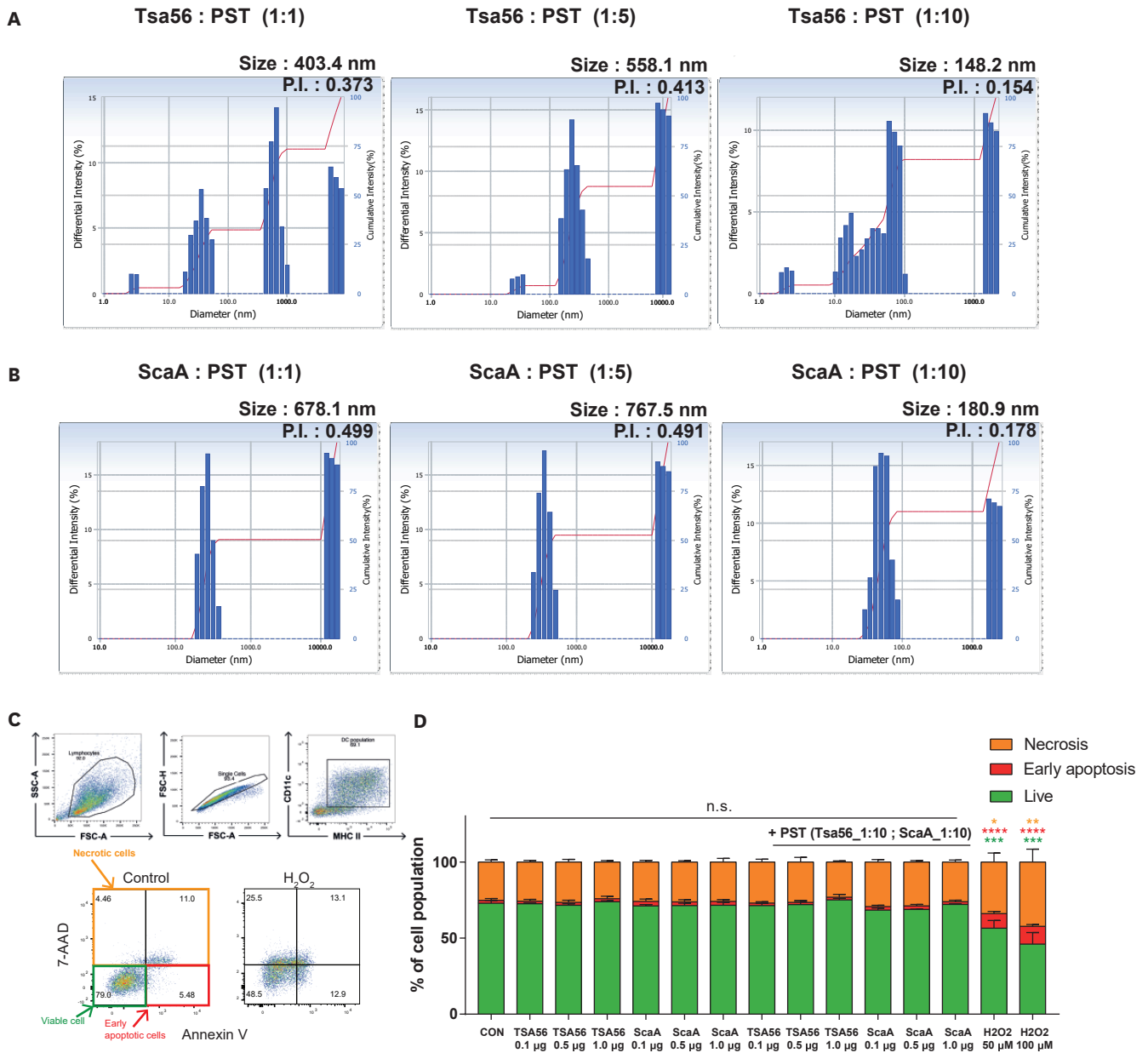


Figure 2. Physicochemical characterization of PST with TSA56 or ScaA. (A, B) PST with TSA56 or ScaA, mixed at weight ratios of 1:1, 1:5, and 1:10, were incubated at room temperature for 30 min to allow complex formation. Size distributions of (A) TSA56-PST and (B) ScaA-PST complexes at different weight ratios were measured by DLS. (C) Gating strategy for cytotoxicity assay. (D) Cytotoxicity of TSA56-PST and ScaA-PST was analyzed in BMDCs stained with annexin V/7-AAD using flow cytometry (n=5). Results are presented as mean ± SEM. Significant differences compared with CON group within each gating (Live, Early apoptosis, Necrosis) determined by *t*-test. **p*<0.05, ***p*<0.01, ****p*<0.001, *****p*<0.0001.

TSA56-PST vaccinated group (Fig. 4D and E). Similarly, the proliferation of CD4⁺ and CD8⁺ T cells was significantly enhanced in the group vaccinated with ScaA-PST (Fig. 4F and G) when restimulated with ScaA. Thus, when complexed with TSA56 or ScaA Ag, PST could enhance CD8⁺ and CD4⁺ T cells responses to the Ag. Collectively, the findings indicated that PST induced increase in both humoral and cellular immune responses, which are essential to confer protective immunity against *O. tsutsugamushi* infection.

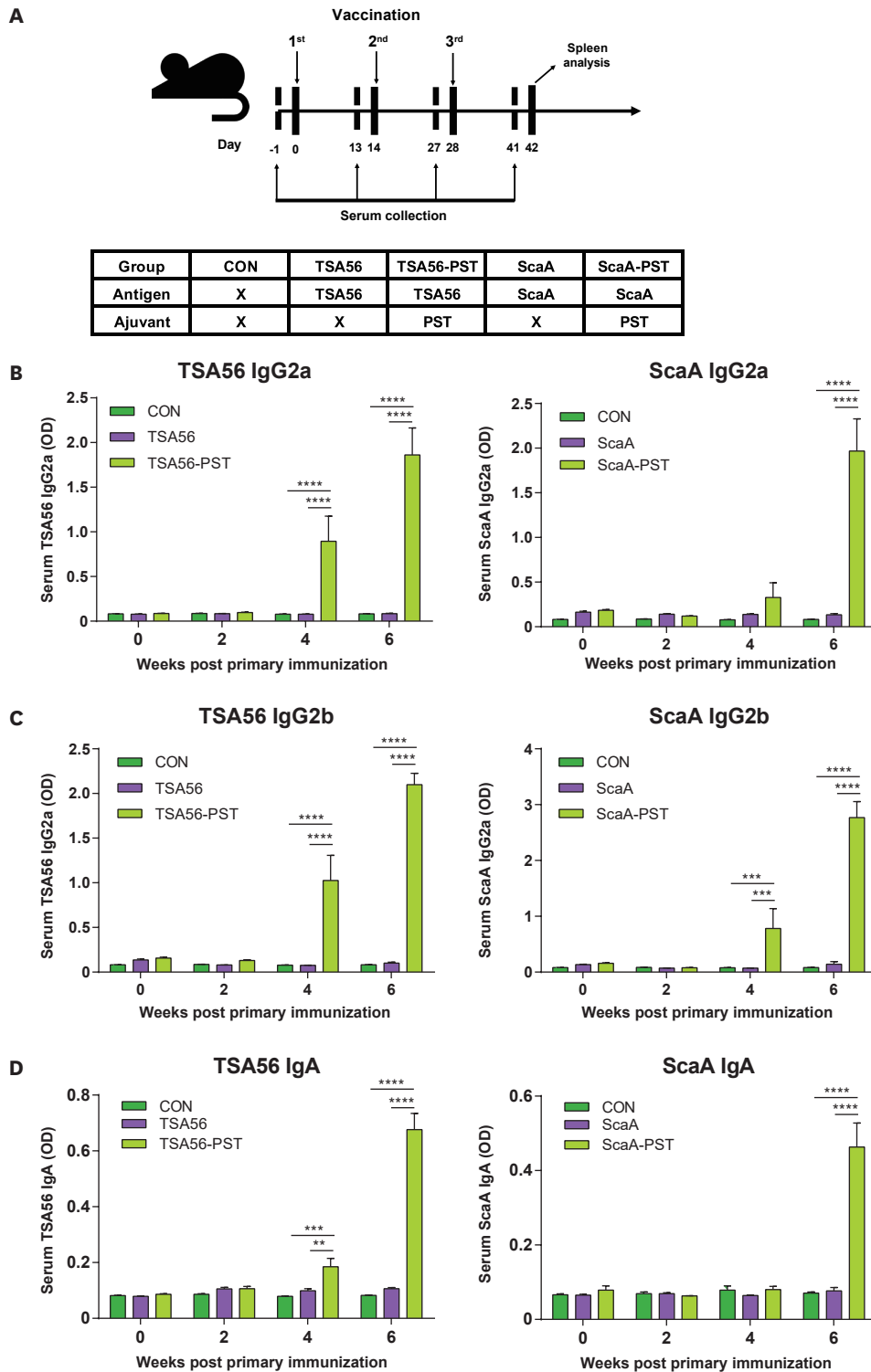


Figure 3. Ag-specific Ab responses in mice immunized with TSA56-PST or ScaA-PST. Mice (n=5 mice/group pooled data from 2 independent experiments) were immunized three times at 2-wk intervals with TSA56, ScaA, TSA56-PST, or ScaA-PST. (A) Schematic of vaccination protocol. TSA56- or ScaA-specific (B) IgG2a, (C) IgG2b, and (D) IgA in serum were determined by ELISA. Results are presented as means \pm SEMs. Significant differences were analyzed by two-way analysis of variance, followed by Tukey's multiple comparison test. Significant difference is noted only within the time points. **p<0.01, ***p<0.001, ****p<0.0001.

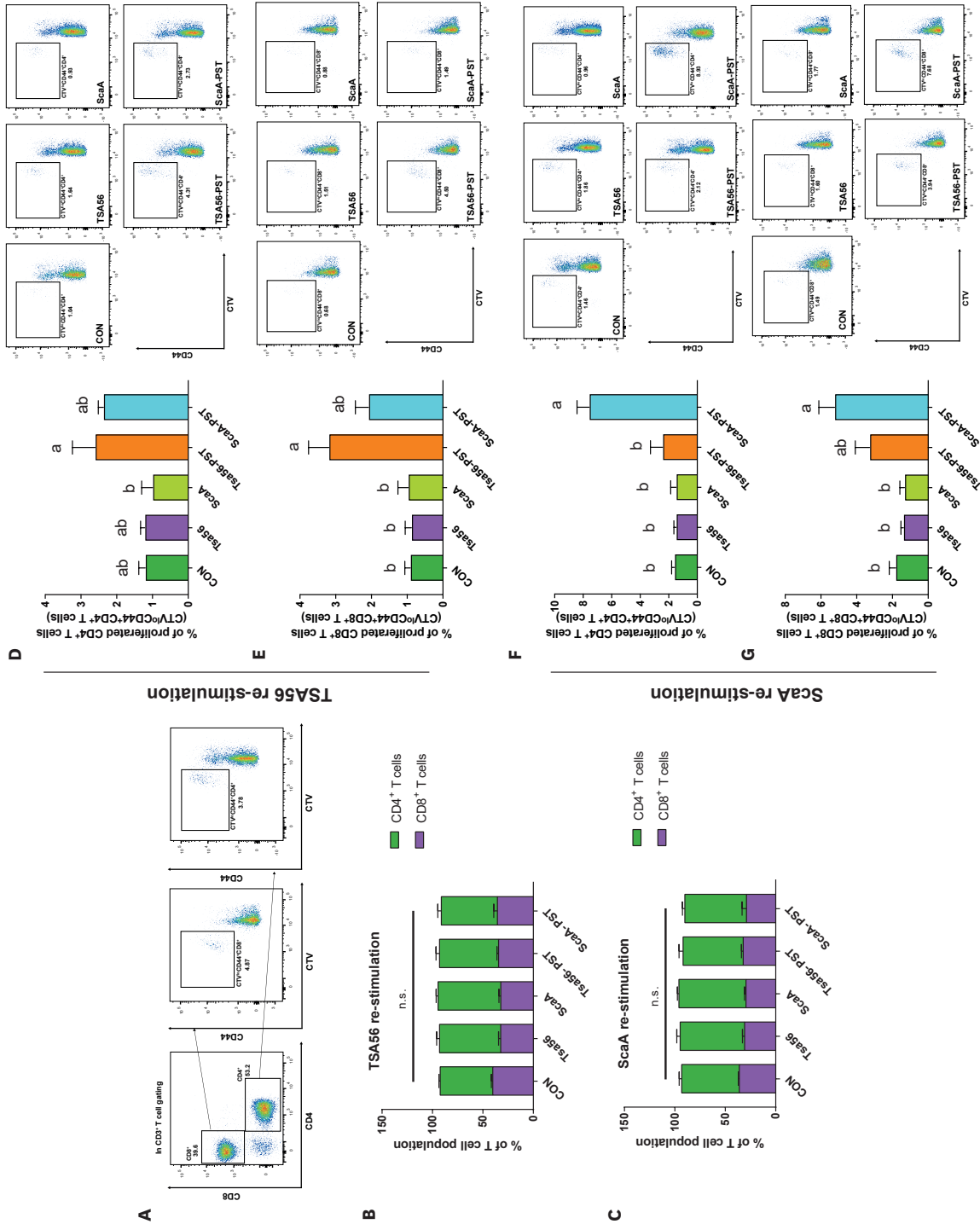


Figure 4. Ag-specific T-cell responses in mice vaccinated with TSA56-PST or ScaA-PST. Mice (n=5 mice/group pooled data from 2 independent experiments) were immunized three times at 2-week interval with TSA56, ScaA, TSA56-PST, or ScaA-PST. Two weeks after the third vaccination, spleens were collected; single cells from splenocytes were labeled with TSA56 or ScaA protein (10 µg/ml) for 72 h. Then, changes in CD4⁺ and CD8⁺ T cell populations were examined by flow cytometry. (A) Gating strategy for the proliferation of CD4⁺ and CD8⁺ T cells. (B, C) The total populations of CD8⁺ and CD4⁺ T cells were examined after (B) TSA56 or (C) ScaA protein restimulation. (D, E) After TSA56 protein restimulation, the changes in proliferation (CTV^{lo}CD44⁺) among (D) CD4⁺ or (E) CD8⁺ T cells were examined. (F, G) After ScaA protein restimulation, the change in proliferation (CTV^{lo}CD44⁺) among (F) CD4⁺ T cells or (G) CD8⁺ T cells were measured. (D-G) Proliferation results are presented with each of the representative dot plot. Results are presented as mean ± SEM. Significant differences were analyzed by one-way ANOVA, followed by Tukey's multiple comparison test. ^{a,b}Different letters indicate statistically significant at p<0.05.

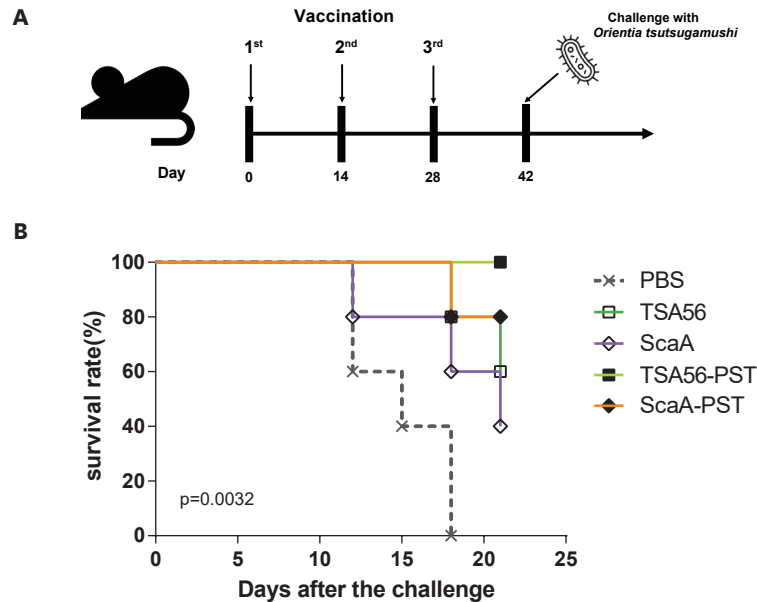


Figure 5. Protective immunity against *O. tsutsugamushi* in mice immunized with TSA56-PST or ScaA-PST. Mice (n=5) were immunized with TSA56, ScaA, TSA56-PST, or ScaA-PST for three times at 2-wk interval. Two weeks after the final immunization, mice were challenged by intraperitoneal infection with *O. tsutsugamushi* Boryong strain (5×10^6 ICU, 100% lethal dose). (A) Schematic vaccination schedule. (B) Survival of mice after the lethal challenge with *O. tsutsugamushi*. Mortality among the group of mice was monitored for 3 weeks; the survival rate was calculated as the ratio of live to total challenged mice within each group. Significant differences in survival rate were determined by the log-rank (Mantel-Cox) test.

Nano-complexed TSA56 and ScaA Ags produced with PST induced protective immunity

Next, we examined whether a vaccine strategy using PST could induce protective immunity against *O. tsutsugamushi* infection. 14 days after the third vaccination, mice were challenged with a lethal dose of *O. tsutsugamushi* (Fig. 5A). No significant weight loss which is considered the end point of experiment was observed during all experimental period. Mice vaccinated with TSA56-PST or ScaA-PST had high survival rates whereas the administration of Ag alone (without PST) resulted in low survival rates (Fig. 5B). In particular, the group vaccinated with TSA56-PST had a 100% survival and the group vaccinated with ScaA-PST had 80% survival throughout the experimental period (Fig. 5B). Collectively, the results indicated that a vaccine strategy that utilizes PST to deliver nano-size target Ags effectively elicits appropriate protective immunity with improved survival against *O. tsutsugamushi* infection.

DISCUSSION

Despite continuous efforts to develop a prophylactic vaccine against *O. tsutsugamushi* infection, a reliable vaccine has not been developed (6). The use of nanotechnology in vaccination strategies has successfully enhanced vaccination efficacy, suggesting a new paradigm for vaccine development (18). Consistent with such applications, we harnessed PST, a nanoparticle-forming transporter, as a delivery agent for intranasal vaccines against *O. tsutsugamushi* infection. We showed that the nano-complexed vaccine Ags, TSA56-PST and ScaA-PST, could elicit protective immunity against lethal *O. tsutsugamushi* infection.

Notably, an intranasal vaccination strategy with PST effectively induced humoral immune responses, including Ag-specific IgA production. The production of IgA is a primary benefit of the vaccination strategy targeting the mucosal area (35,36). In our previous studies, intranasal vaccination with PST also showed a protective immune response against respiratory syncytial virus infection and pneumonia, with effective production of IgA (19,20). While *O. tsutsugamushi* infection gives rise to typically vasculitis in human, the current murine infection model utilizes an intraperitoneal route of inoculation (37). Even those *O. tsutsugamushi* infections does not directly occur through the respiratory system, it has been discovered recently that *O. tsutsugamushi* infection causes lung inflammation that is often followed by endothelial dysfunction (38,39). Furthermore, as we previously reported (6), intranasal immunization showed much higher IgA levels resulting superior protection to other systemic routes (subcutaneous or intraperitoneal). Therefore, the production of IgA by PST is a factor that contributes to protective immunity against *O. tsutsugamushi* infection.

Because *O. tsutsugamushi* is an obligate intracellular bacterium, *O. tsutsugamushi* infections are difficult to effectively control by humoral immunity alone. Cellular immunity, which can directly kill infected cells, must therefore be accompanied by Ab production (22,40). Until recently, vaccine development primarily focused on increases in Ab production, rather than enhancement of cellular immunity, partly because Ab production is the standard parameter measured in clinical trials. Insufficient T cell response induction is primary obstacles in protective vaccine development against *O. tsutsugamushi* infection (5,41). The accompanying Ag specific CD8⁺ and CD4⁺ T cell responses when using nano-complexed *O. tsutsugamushi* proteins produced with PST were presumably key factors for protective immunity. After the third vaccination, both CD8⁺ and CD4⁺ T cell responses were observed upon restimulation. The proliferation of T cells increased only when the restimulation Ag was identical to the vaccine Ag. Therefore, the T cell response confirmed in the present study was not a bystander effect related to the low immunogenicity of purified TSA56 and ScaA proteins. CD8⁺ T cells play an essential role in cellular immunity by transitioning into cytotoxic T lymphocytes, which directly eliminate infected cells (42,43). Cytotoxic T lymphocyte function is dependent on the production of IFN- γ , which directly enhances the motility and cytotoxicity of cytotoxic T lymphocytes (29,44). In addition, it is well described that the expression of granzyme B, perforin and CD107a play a critical role in function of CD8⁺ T cells (45-47). Additionally, CD4⁺ T cells can function as helper T cells to assist CD8⁺ T cell responses. In particular, IFN- γ from CD4⁺ T cells is necessary for host survival and enhances CD8⁺ T cell function during infection (48,49). Here, we found that nano-complexed TSA56 or ScaA vaccine with PST could generate memory CD4⁺ and CD8⁺ T cells. Generation of memory T cells in addition to the Ag-specific Ab formation after the vaccination could be a key strategy in vaccine development not only against *O. tsutsugamushi* but also any other intracellular pathogen because it is important asset to eliminate infected cells. Therefore, it is necessary to conduct further study to examine how nano-complexed vaccine with PST affects the function of memory T cells including the expression of IFN- γ and granzymes.

The mediation of APCs is essential for Ag-specific T cell responses because APCs process internalized Ags and present appropriate epitopes to T cells. The T cell responses to *O. tsutsugamushi* confirmed in this study may also be mediated by APCs. Among the APCs, DCs play a key role in the activation of naïve T cells by presenting a cognate Ag loaded on MHC molecules (50). DCs have 2 major pathways for Ag presentation to CD8⁺ and CD4⁺ T cells, depending on Ag origin (51). First, they can present intracellular endogenous Ags loaded on MHC class I molecules, resulting in CD8⁺ T cell activation (52). In contrast, after exogenous

Ag-derived peptides have been internalized, they are loaded on MHC class II molecules; presentation of Ags on these MHC molecules results in CD4⁺ T cell responses (53). To induce appropriate CD8⁺ T cell responses from exogenous Ags, DC must present exogenous Ags through MHC class I molecules by a mechanism known as cross-presentation. Because most vaccine Ags encounter DCs in the extracellular environment, cross-presentation plays a major role in activating CD8⁺ T cells to manage viral and intracellular bacterial infections (54-57).

Because PST enhanced the CD8⁺ T cell responses against TSA56 and ScaA proteins in the present study, PST is likely to be involved in the cross-presentation ability of DCs. We previously reported that PST had a proton-sponge effect, which modulated the intracellular Ag mobility (19). Moreover, the proton-sponge effect has the potential to enhance cross-presentation (18). It may be necessary to investigate whether PST can modulate the cross-presentation of TSA56 and ScaA Ags in DCs.

In conclusion, we demonstrated that nano-size vaccines produced with PST induced Ag-specific Ab responses (including IgG and IgA) to target proteins. Moreover, the vaccines induced Ag specific CD4⁺ and CD8⁺ T cell responses, including cell proliferation. Finally, the promotion of both humoral and cellular immunity resulted in protective immunity against *O. tsutsugamushi* infection. Overall, our findings suggest that an intranasal vaccination strategy using PST as a nano-size delivery agent can provide effective protection against *O. tsutsugamushi* infection.

ACKNOWLEDGEMENTS

This research was supported by the Korea Initiative for Fostering University Research and Innovation Program of the National Research Foundation (NRF), funded by the Korean government (MSIT) (No. NRF-2020M3H1A1073304) and a National Institutes of Health research project (2021-NI-013-00). This work also received partial support from the Ministry of Health & Welfare (HV22C0183), Republic of Korea. The study was also partially supported by the BK21 FOUR Program of the Department of Agricultural Biotechnology, Seoul National University, Seoul, Korea.

REFERENCES

1. Xu G, Walker DH, Jupiter D, Melby PC, Arcari CM. A review of the global epidemiology of scrub typhus. *PLoS Negl Trop Dis* 2017;11:e0006062.
[PUBMED](#) | [CROSSREF](#)
2. Luce-Fedrow A, Lehman ML, Kelly DJ, Mullins K, Maina AN, Stewart RL, Ge H, John HS, Jiang J, Richards AL. A review of scrub typhus (*Orientia tsutsugamushi* and related organisms): then, now, and tomorrow. *Trop Med Infect Dis* 2018;3:8.
[PUBMED](#) | [CROSSREF](#)
3. Kala D, Gupta S, Nagraik R, Verma V, Thakur A, Kaushal A. Diagnosis of scrub typhus: recent advancements and challenges. *J Biotech* 2020;10:396.
[PUBMED](#) | [CROSSREF](#)
4. Banerjee A, Kulkarni S. *Orientia tsutsugamushi*: the dangerous yet neglected foe from the East. *Int J Med Microbiol* 2021;311:151467.
[PUBMED](#) | [CROSSREF](#)
5. Valbuena G, Walker DH. Approaches to vaccines against *Orientia tsutsugamushi*. *Front Cell Infect Microbiol* 2013;2:170.
[PUBMED](#) | [CROSSREF](#)

6. Park SM, Gu MJ, Ju YJ, Cheon IS, Hwang KJ, Gill B, Shim BS, Jeong HJ, Son YM, Choi S, et al. Intranasal vaccination with outer-membrane protein of *Orientia tsutsugamushi* induces protective immunity against scrub typhus. *Immune Netw* 2020;21:e14.
[PUBMED](#) | [CROSSREF](#)
7. Basharat Z, Akhtar U, Khan K, Alotaibi G, Jalal K, Abbas MN, Hayat A, Ahmad D, Hassan SS. Differential analysis of *Orientia tsutsugamushi* genomes for therapeutic target identification and possible intervention through natural product inhibitor screening. *Comput Biol Med* 2022;141:105165.
[PUBMED](#) | [CROSSREF](#)
8. Ha NY, Sharma P, Kim G, Kim Y, Min CK, Choi MS, Kim IS, Cho NH. Immunization with an autotransporter protein of *Orientia tsutsugamushi* provides protective immunity against scrub typhus. *PLoS Negl Trop Dis* 2015;9:e0003585.
[PUBMED](#) | [CROSSREF](#)
9. Ha NY, Shin HM, Sharma P, Cho HA, Min CK, Kim HI, Yen NT, Kang JS, Kim IS, Choi MS, et al. Generation of protective immunity against *Orientia tsutsugamushi* infection by immunization with a zinc oxide nanoparticle combined with ScaA antigen. *J Nanobiotechnology* 2016;14:76.
[PUBMED](#) | [CROSSREF](#)
10. Kim HI, Ha NY, Kim G, Min CK, Kim Y, Yen NT, Choi MS, Cho NH. Immunization with a recombinant antigen composed of conserved blocks from TSA56 provides broad genotype protection against scrub typhus. *Emerg Microbes Infect* 2019;8:946-958.
[PUBMED](#) | [CROSSREF](#)
11. Chattopadhyay S, Richards AL. Scrub typhus vaccines: past history and recent developments. *Hum Vaccin* 2007;3:73-80.
[PUBMED](#) | [CROSSREF](#)
12. Koralur MC, Ramaiah A, Dasch GA. Detection and distribution of Sca autotransporter protein antigens in diverse isolates of *Orientia tsutsugamushi*. *PLoS Negl Trop Dis* 2018;12:e0006784.
[PUBMED](#) | [CROSSREF](#)
13. Cho BA, Cho NH, Seong SY, Choi MS, Kim IS. Intracellular invasion by *Orientia tsutsugamushi* is mediated by integrin signaling and actin cytoskeleton rearrangements. *Infect Immun* 2010;78:1915-1923.
[PUBMED](#) | [CROSSREF](#)
14. Lee JH, Cho NH, Kim SY, Bang SY, Chu H, Choi MS, Kim IS. Fibronectin facilitates the invasion of *Orientia tsutsugamushi* into host cells through interaction with a 56-kDa type-specific antigen. *J Infect Dis* 2008;198:250-257.
[PUBMED](#) | [CROSSREF](#)
15. Cai T, Liu H, Zhang S, Hu J, Zhang L. Delivery of nanovaccine towards lymphoid organs: recent strategies in enhancing cancer immunotherapy. *J Nanobiotechnology* 2021;19:389.
[PUBMED](#) | [CROSSREF](#)
16. Zhang Y, Lin S, Wang XY, Zhu G. Nanovaccines for cancer immunotherapy. *Wiley Interdiscip Rev Nanomed Nanobiotechnol* 2019;11:e1559.
[PUBMED](#) | [CROSSREF](#)
17. Jiang H, Wang Q, Sun X. Lymph node targeting strategies to improve vaccination efficacy. *J Control Release* 2017;267:47-56.
[PUBMED](#) | [CROSSREF](#)
18. Kim CG, Kye YC, Yun CH. The role of nanovaccine in cross-presentation of antigen-presenting cells for the activation of CD8⁺ T cell responses. *Pharmaceutics* 2019;11:612.
[PUBMED](#) | [CROSSREF](#)
19. Firdous J, Islam MA, Park SM, Cheon IS, Shim BS, Yoon HS, Song M, Chang J, Choi YJ, Park YM, et al. Induction of long-term immunity against respiratory syncytial virus glycoprotein by an osmotic polymeric nanocarrier. *Acta Biomater* 2014;10:4606-4617.
[PUBMED](#) | [CROSSREF](#)
20. Kye YC, Park SM, Shim BS, Firdous J, Kim G, Kim HW, Ju YJ, Kim CG, Cho CS, Kim DW, et al. Intranasal immunization with pneumococcal surface protein A in the presence of nanoparticle forming polysorbitol transporter adjuvant induces protective immunity against the *Streptococcus pneumoniae* infection. *Acta Biomater* 2019;90:362-372.
[PUBMED](#) | [CROSSREF](#)
21. Paramithiotis E, Sugden S, Papp E, Bonhomme M, Chermak T, Crawford SY, Demetriades SZ, Galdos G, Lambert BL, Mattison J, et al. Cellular immunity is critical for assessing COVID-19 vaccine effectiveness in immunocompromised individuals. *Front Immunol* 2022;13:880784.
[PUBMED](#) | [CROSSREF](#)
22. Griffiths KL, Khader SA. Novel vaccine approaches for protection against intracellular pathogens. *Curr Opin Immunol* 2014;28:58-63.
[PUBMED](#) | [CROSSREF](#)

23. Hauptmann M, Kolbaum J, Lilla S, Wozniak D, Gharaibeh M, Fleischer B, Keller CA. Protective and pathogenic roles of CD8⁺ T lymphocytes in murine *Orientia tsutsugamushi* infection. *PLoS Negl Trop Dis* 2016;10:e0004991.
[PUBMED](#) | [CROSSREF](#)
24. Xu G, Mendell NL, Liang Y, Shelite TR, Goez-Rivillas Y, Soong L, Bouyer DH, Walker DH. CD8⁺ T cells provide immune protection against murine disseminated endotheliotropic *Orientia tsutsugamushi* infection. *PLoS Negl Trop Dis* 2017;11:e0005763.
[PUBMED](#) | [CROSSREF](#)
25. Kim HW, Ju DB, Kye YC, Ju YJ, Kim CG, Lee IK, Park SM, Choi IS, Cho KK, Lee SH, et al. Galectin-9 induced by dietary probiotic mixture regulates immune balance to reduce atopic dermatitis symptoms in mice. *Front Immunol* 2020;10:3063.
[PUBMED](#) | [CROSSREF](#)
26. Chu H, Park SM, Cheon IS, Park MY, Shim BS, Gil BC, Jeung WH, Hwang KJ, Song KD, Hong KJ, et al. *Orientia tsutsugamushi* infection induces CD4⁺ T cell activation via human dendritic cell activity. *J Microbiol Biotechnol* 2013;23:1159-1166.
[PUBMED](#) | [CROSSREF](#)
27. Tamura A, Urakami H. Easy method for infectivity titration of *Rickettsia tsutsugamushi* by infected cell counting. *Nippon Saikingaku Zasshi* 1981;36:783-785.
[PUBMED](#) | [CROSSREF](#)
28. Min CK, Kim HI, Ha NY, Kim Y, Kwon EK, Yen NT, Youn JI, Jeon YK, Inn KS, Choi MS, et al. A type I interferon and IL-10 induced by *Orientia tsutsugamushi* infection suppresses antigen-specific T cells and their memory responses. *Front Immunol* 2018;9:2022.
[PUBMED](#) | [CROSSREF](#)
29. Bhat P, Leggatt G, Waterhouse N, Frazer IH. Interferon- γ derived from cytotoxic lymphocytes directly enhances their motility and cytotoxicity. *Cell Death Dis* 2017;8:e2836.
[PUBMED](#) | [CROSSREF](#)
30. Sumonwiriya M, Paris DH, Sunyakumthorn P, Anantatat T, Jenjaroen K, Chumseng S, Im-Erbsin R, Tanganuchitcharnchai A, Jintaworn S, Blacksell SD, et al. Strong interferon-gamma mediated cellular immunity to scrub typhus demonstrated using a novel whole cell antigen ELISpot assay in rhesus macaques and humans. *PLoS Negl Trop Dis* 2017;11:e0005846.
[PUBMED](#) | [CROSSREF](#)
31. Seong SY, Choi MS, Kim IS. *Orientia tsutsugamushi* infection: overview and immune responses. *Microbes Infect* 2001;3:11-21.
[PUBMED](#) | [CROSSREF](#)
32. Farber DL, Yudanin NA, Restifo NP. Human memory T cells: generation, compartmentalization and homeostasis. *Nat Rev Immunol* 2014;14:24-35.
[PUBMED](#) | [CROSSREF](#)
33. Sasaki K, Moussawy MA, Abou-Daya KI, Macedo C, Hosni-Ahmed A, Liu S, Juya M, Zahorchak AF, Metes DM, Thomson AW, et al. Activated-memory T cells influence naïve T cell fate: a noncytotoxic function of human CD8 T cells. *Commun Biol* 2022;5:634.
[PUBMED](#) | [CROSSREF](#)
34. Tarke A, Coelho CH, Zhang Z, Dan JM, Yu ED, Methot N, Bloom NI, Goodwin B, Phillips E, Mallal S, et al. SARS-CoV-2 vaccination induces immunological T cell memory able to cross-recognize variants from Alpha to Omicron. *Cell* 2022;185:847-859.e11.
[PUBMED](#) | [CROSSREF](#)
35. Hemmi T, Aina A, Hashiguchi T, Tobiume M, Kanno T, Iwata-Yoshikawa N, Iida S, Sato Y, Miyamoto S, Ueno A, et al. Intranasal vaccination induced cross-protective secretory IgA antibodies against SARS-CoV-2 variants with reducing the potential risk of lung eosinophilic immunopathology. *Vaccine* 2022;40:5892-5903.
[PUBMED](#) | [CROSSREF](#)
36. Li L, Wang M, Hao J, Han J, Fu T, Bai J, Tian M, Jin N, Zhu G, Li C. Mucosal IgA response elicited by intranasal immunization of *Lactobacillus plantarum* expressing surface-displayed RBD protein of SARS-CoV-2. *Int J Biol Macromol* 2021;190:409-416.
[PUBMED](#) | [CROSSREF](#)
37. Shelite TR, Saito TB, Mendell NL, Gong B, Xu G, Soong L, Valbuena G, Bouyer DH, Walker DH. Hematogenously disseminated *Orientia tsutsugamushi*-infected murine model of scrub typhus [corrected]. *PLoS Negl Trop Dis* 2014;8:e2966.
[PUBMED](#) | [CROSSREF](#)
38. Trent B, Fisher J, Soong L. Scrub Typhus Pathogenesis: Innate Immune Response and Lung Injury During *Orientia tsutsugamushi* Infection. *Front Microbiol* 2019;10:2065.
[PUBMED](#) | [CROSSREF](#)

39. Trent B, Liang Y, Xing Y, Esqueda M, Wei Y, Cho NH, Kim HI, Kim YS, Shelite TR, Cai J, et al. Polarized lung inflammation and Tie2/angiopoietin-mediated endothelial dysfunction during severe *Orientia tsutsugamushi* infection. *PLoS Negl Trop Dis* 2020;14:e0007675.
[PUBMED](#) | [CROSSREF](#)
40. Atwal S, Wongsantichon J, Giengkam S, Saharat K, Pittayasathornthun YJ, Chuenklin S, Wang LC, Chung T, Huh H, Lee SH, et al. The obligate intracellular bacterium *Orientia tsutsugamushi* differentiates into a developmentally distinct extracellular state. *Nat Commun* 2022;13:3603.
[PUBMED](#) | [CROSSREF](#)
41. Liu J, Chandrashekar A, Sellers D, Barrett J, Jacob-Dolan C, Lifton M, McMahan K, Sciacca M, VanWyk H, Wu C, et al. Vaccines elicit highly conserved cellular immunity to SARS-CoV-2 Omicron. *Nature* 2022;603:493-496.
[PUBMED](#) | [CROSSREF](#)
42. Farhood B, Najafi M, Mortezaee K. CD8⁺ cytotoxic T lymphocytes in cancer immunotherapy: a review. *J Cell Physiol* 2019;234:8509-8521.
[PUBMED](#) | [CROSSREF](#)
43. Kuznetsova M, Lopatnikova J, Shevchenko J, Silkov A, Maksyutov A, Sennikov S. Cytotoxic activity and memory T cell subset distribution of *in vitro*-stimulated CD8⁺ T cells specific for HER2/neu epitopes. *Front Immunol* 2019;10:1017.
[PUBMED](#) | [CROSSREF](#)
44. Hillaire ML, Lawrence P, Lagrange B. IFN- γ : a crucial player in the fight against HBV infection? *Immune Netw* 2023;23:e30.
[PUBMED](#) | [CROSSREF](#)
45. Kiniry BE, Hunt PW, Hecht FM, Somsouk M, Deeks SG, Shacklett BL. Differential expression of CD8⁺ T cell cytotoxic effector molecules in blood and gastrointestinal mucosa in HIV-1 infection. *J Immunol* 2018;200:1876-1888.
[PUBMED](#) | [CROSSREF](#)
46. Zöphel D, Angenendt A, Kaschek L, Ravichandran K, Hof C, Janku S, Hoth M, Lis A. Faster cytotoxicity with age: Increased perforin and granzyme levels in cytotoxic CD8⁺ T cells boost cancer cell elimination. *Aging Cell* 2022;21:e13668.
[PUBMED](#) | [CROSSREF](#)
47. Aktas E, Kucuksezer UC, Bilgic S, Erten G, Deniz G. Relationship between CD107a expression and cytotoxic activity. *Cell Immunol* 2009;254:149-154.
[PUBMED](#) | [CROSSREF](#)
48. Green AM, Difazio R, Flynn JL. IFN- γ from CD4 T cells is essential for host survival and enhances CD8 T cell function during *Mycobacterium tuberculosis* infection. *J Immunol* 2013;190:270-277.
[PUBMED](#) | [CROSSREF](#)
49. Topchyan P, Lin S, Cui W. The role of CD4 T cell help in CD8 T cell differentiation and function during chronic infection and cancer. *Immune Netw* 2023;23:e41.
[PUBMED](#) | [CROSSREF](#)
50. Bousso P. T-cell activation by dendritic cells in the lymph node: lessons from the movies. *Nat Rev Immunol* 2008;8:675-684.
[PUBMED](#) | [CROSSREF](#)
51. Guermonprez P, Valladeau J, Zitvogel L, Théry C, Amigorena S. Antigen presentation and T cell stimulation by dendritic cells. *Annu Rev Immunol* 2002;20:621-667.
[PUBMED](#) | [CROSSREF](#)
52. Pooley JL, Heath WR, Shortman K. Cutting edge: intravenous soluble antigen is presented to CD4 T cells by CD8⁺ dendritic cells, but cross-presented to CD8 T cells by CD8⁺ dendritic cells. *J Immunol* 2001;166:5327-5330.
[PUBMED](#) | [CROSSREF](#)
53. Gerner MY, Casey KA, Mescher MF. Defective MHC class II presentation by dendritic cells limits CD4 T cell help for antitumor CD8 T cell responses. *J Immunol* 2008;181:155-164.
[PUBMED](#) | [CROSSREF](#)
54. Joffre OP, Segura E, Savina A, Amigorena S. Cross-presentation by dendritic cells. *Nat Rev Immunol* 2012;12:557-569.
[PUBMED](#) | [CROSSREF](#)
55. Alloatti A, Kotsias F, Magalhaes JG, Amigorena S. Dendritic cell maturation and cross-presentation: timing matters! *Immunol Rev* 2016;272:97-108.
[PUBMED](#) | [CROSSREF](#)
56. Embgenbroich M, Burgdorf S. Current concepts of antigen cross-presentation. *Front Immunol* 2018;9:1643.
[PUBMED](#) | [CROSSREF](#)
57. Gros M, Amigorena S. Regulation of antigen export to the cytosol during cross-presentation. *Front Immunol* 2019;10:41.
[PUBMED](#) | [CROSSREF](#)